Scientific Journal of Astana IT University
ISSN (P): 2707-9031 ISSN (E): 2707-904X
VOLUME 23, SEPTEMBER 2025

DOI: 10.37943/23FVQL2644

Perizat Omarova
PhD, Department of Computer Science
omarova.peryzat2@gmail.com, orcid.org/0000-0001-9502-7959
Al-Farabi Kazakh National University, Kazakhstan
Institute Of Information and Computational Technology, Kazakhstan

Alexandr Neftissov
PhD, Associate Professor, Rectorate for Science and Innovation
alexandr.neftissov@astanait.edu.kz, orcid.org/0000-0003-4079-2025
Academy of Physical Education and Mass Sports, Kazakhstan
PhD, Associate Professor, Researcher, Scientific-Innovation Center Industry 4.0
Astana IT University, Kazakhstan

Aliya Borsikbayeva
Master's degree, School of Applied Mathematics
borsikbayeva.aliya18@gmail.com, orcid.org/0009-0000-1039-8137
Kazakh-British Technical University, Kazakhstan

Ilyas Kazambayev
Master`s degree, Acting Director of Scientific-Innovation Center Industry 4.0
i.kazambayev@astanait.edu.kz, orcid.org/0000-0003-0850-7490
Astana IT University, Kazakhstan

Artem Biloshchytskyi
Bachelor's student, School of Computer Engineering
baa20.10.2005@gmail.com, orcid.org/0009-0000-5571-4412

Aliya Aubakirova*
PhD student, Junior Researcher of Scientific-Innovation Center Industry 4.0
aliya.aubakirova@astanait.edu.kz, orcid.org/0009-0004-6925-6714
Astana IT University, Kazakhstan

NUMERICAL SIMULATION OF WATER FLOW THROUGH A POROUS MEDIUM: VERIFICATION BY THE LIN 1999 EXPERIMENT

Abstract: The presented study verifies a numerical model of fluid flow through a porous structure based on the experiment by Lin (1999). Water flows through porous media with a free surface are common in hydraulic engineering applications, such as dam breaks, seepage through dams, and the operation of wave protection structures. For a more accurate forecast, numerical modeling and verification should be performed using reliable experimental data. The experiment studied flow motion after a sudden removal of a partition (analogous to a dam break) in a rectangular channel with a porous obstacle. The laboratory setup had dimensions of 0.892 m × 0.37 m × 0.44 m, and the porous insert of 0.29 m × 0.37 m × 0.44 m was placed in a section of 0.3–0.59 m along the X-axis. Thus, the porous barrier blocked the cross-section of the channel, and water could flow only through its pores. This work helps to convey the forecast and allows to adequately simulate natural "jams" of branches and stones. This work demonstrates how, using such a verified model, it is possible to predict the flow dynamics in real conditions: water level changes, velocity field and coastal sediment accumulation zones. In addition, obtained data can serve as a basis for early warning of environmental risks and

Received: 11.08.2025 Accepted: 24.09.2025 Published: 30.09.2025

DOI: 10.37943/23FVQL2644

development of measures to protect water resources. In the future, it is planned to apply the model to a real section of the Talas River for a more detailed and reliable assessment of water pollution processes.

Keywords: porous media; numerical simulation; damb break, river pollution, water level.

Introduction

Water is one of the vital resources of the environment. The daily aggravation of the problem of water shortage provides for the introduction of state-of-the-art methods aimed at increasing water productivity in agriculture, which results in an increase in the amount of crop yield while reducing the amount of water used [1]. Other important problems related to water resources are floods and breakthroughs of hydraulic structures [2], siltation, water pollution, etc. Floods caused by breakthroughs of hydraulic structures are of particular interest, since such a natural disaster is associated with a complex geographical landscape of rivers and lakes. The main cause of the increasing frequency of floods at the global level is global climate change and human activities [3], [4].

Despite the high cost and expense of the process, there are experimental data on water resources in the literature [5], [6], [7]. Such works allow us to verify the numerical studies conducted, the developed numerical models, and also provide an opportunity to better understand the dynamics of the fluid flow. Laboratory experiments allow us to study the propagation of flood waves. For example, in the study [8], the authors conducted an experiment consisting of the propagation of three types of Newtonian fluid (water, water with salt, and sunflower oil) along a rectangular installation. Conducting laboratory experiments made it possible to determine the difference between bottom sediments of different and the same diameters [9], [10] experimentally investigated the erosion process to accurately and quickly predict the outflow rate of water after the break of landslide dams. In the paper [11], field experiments were conducted on flushing a reservoir covered with bottom sediments.

Over the past decade, forecasting various events and outcomes has become possible thanks to numerical modeling. The choice of numerical modeling is explained by its availability, low resource consumption and relatively low costs. To obtain the most reliable results, artificial intelligence, remote sensing (ERS), Unmanned Aerial Vehicles (UAVs) and real data obtained from hydroposts jointly with the republican state enterprise "Kazhydromet" and the republican state enterprise "Kazvodkhoz" are also actively used. The reasonableness, accuracy and reliability of the developed models are tested by comparing the obtained results with experimental data [12].

The presented process of the system functioning is an end-to-end sequence of operations, ensuring the transition from the collection of initial information to the formation of analytical conclusions and their provision to end users (Figure 1). At the first stage, a comprehensive collection of data is carried out, including physical parameters, geographic information and hydrological indicators. The obtained information undergoes integration and preliminary processing in order to bring it to a single format and structure necessary for further modeling.

The second stage is implemented within the backend system, where data is received by the recording service and stored in the PostgreSQL relational database. Here, key analytical processing is performed, including multi-scale assessment and numerical modeling of hydrodynamic processes using k-ε and k-ω turbulence models. Based on the obtained results, a comparison with experimental data is performed, verification of calculation models and an assessment of their adequacy are carried out. The constructed CFD models undergo a post-processing stage, including analysis of contour distributions, profiles and multivariate statistical analysis.

Scientific Journal of Astana IT University
ISSN (P): 2707-9031 ISSN (E): 2707-904X
VOLUME 23, SEPTEMBER 2025

The final stage involves publishing the results via API Gateway, making them available to both external systems and frontend interfaces. The client side includes functions for monitoring indicators in real time, conducting analytics, and generating reports [13].

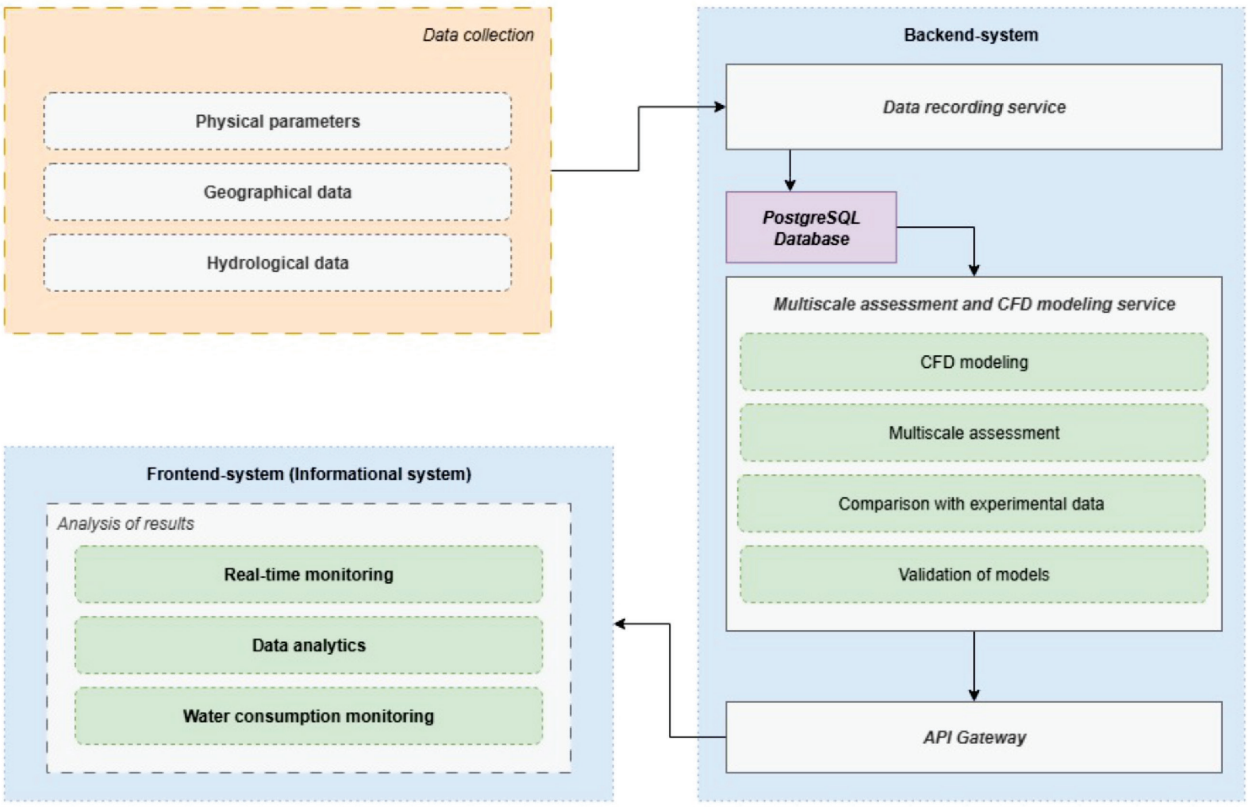

Figure 1. Integrated architecture for data acquisition, validation and CFD modeling

Research area and data

This paper examines the verification of a numerical model of fluid flow through a porous structure based on an experiment, which is planned to be applied in the future to the Talas River flowing through the Zhambyl region of Kazakhstan. It is worth noting that the Talas River is one of the most polluted water bodies in the country (Figure 2). According to the Ministry of Water Resources and Irrigation of the Republic of Kazakhstan, Talas is one of the rivers whose water quality does not meet sanitary standards and is not suitable for most activities. As is known, the main pollutants of the river are suspended matter, salt ions (magnesium, chlorides, calcium, sulfates) and heavy metals (cadmium, manganese, copper, zinc). Thus, pollutants have a negative impact on the river ecosystem, interfere with the photosynthesis of aquatic plants and can cause corrosion of equipment.

One of the reasons for the deterioration of water quality is the ineffectiveness of wastewater treatment facilities in the cities along the river. The deplorable state of these facilities leads to the discharge of untreated wastewater into the river, which exacerbates the pollution problem. In addition, the transboundary nature of the Talas River complicates water management, since water comes from Kyrgyzstan, and any changes in water supply from there directly affect the situation in Kazakhstan.

Improving the water quality in the Talas River requires a comprehensive solution, including upgrading treatment facilities, effective water management, and international cooperation with neighboring countries. Regular water quality monitoring and the development of programs to restore the river's ecosystem are also important steps.

DOI: 10.37943/23FVQL2644

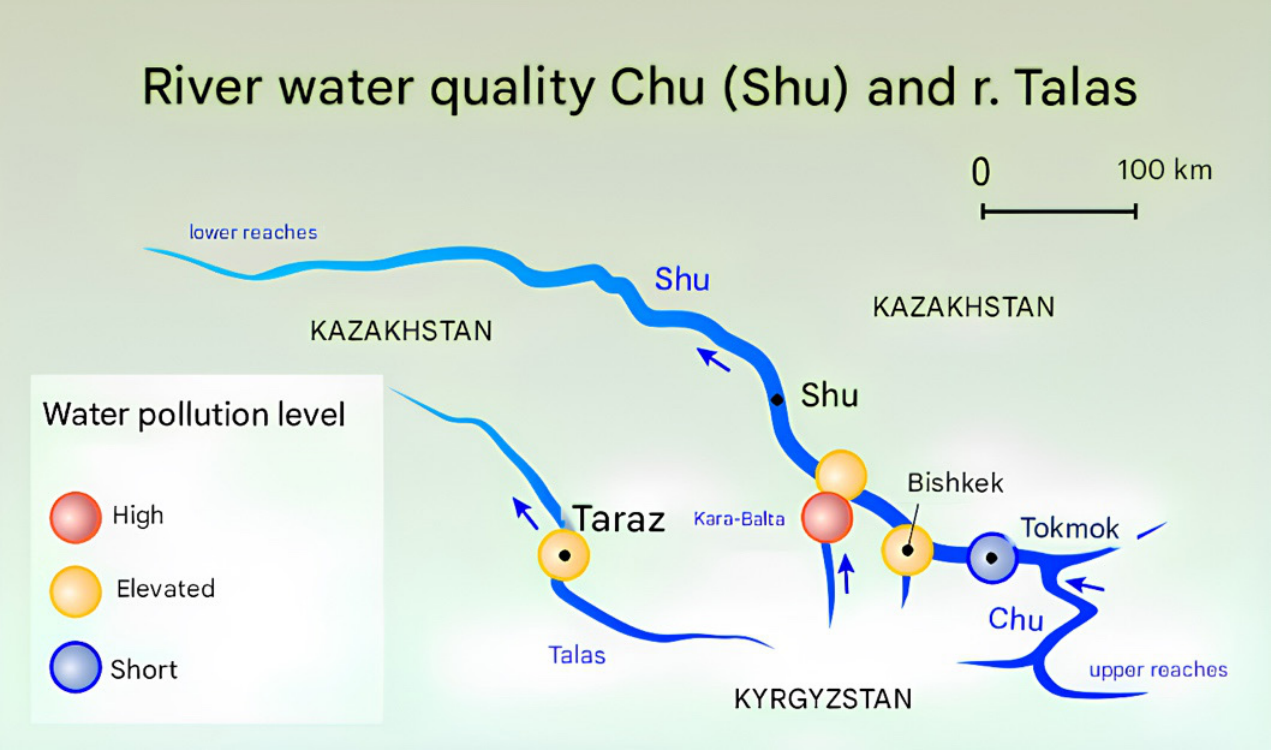

Figure 2. Pollution map of the Shu and Talas rivers [14]

As is known, the Talas River and the Chu River are transboundary watercourses flowing through the territory of Kyrgyzstan and Kazakhstan. The Talas River originates on the northern slopes of the Talas Alatau ridge, its length is about 661 km, and the basin area is over 52,000 km². The river is subject to anthropogenic impact along most of its course, especially in the lower reaches, where there is a partial or complete loss of flow due to intensive water intake for irrigation purposes.

The Chu River, over 1,060 km long, is formed at the confluence of the Dzhuungart and Chon-Kemin rivers in the foothills of the Tien Shan and crosses the Chui Valley, one of the most populated and economically developed regions of Kyrgyzstan and southern Kazakhstan. In the lower reaches, on the territory of Kazakhstan, a significant part of the river's waters is lost in the sands of the Moiynkum Desert, before reaching its final reservoir.

Both rivers have a pronounced flood regime caused by the melting of snow and glaciers in the spring and summer, which significantly affects the concentrations of pollutants in different seasons. Moreover, the main sources of pollution of the Talas River are the former sources of pollution and as a result greatly affect the flow of water, changing its channel and leading to marfological changes.

Based on the study area and the need to take measures to improve transboundary watercourse management, a detailed description of the conceptual framework of the study is provided below (Figure 3). It highlights five key stages, each of which plays its role in building a reliable and verified numerical model and subsequent analysis of the results. Thus, the proposed conceptual framework provides a systematic approach from collecting field data to developing practical recommendations, combining experimental studies, numerical modeling and statistical analysis.

Scientific Journal of Astana IT University
ISSN (P): 2707-9031 ISSN (E): 2707-904X
VOLUME 23, SEPTEMBER 2025

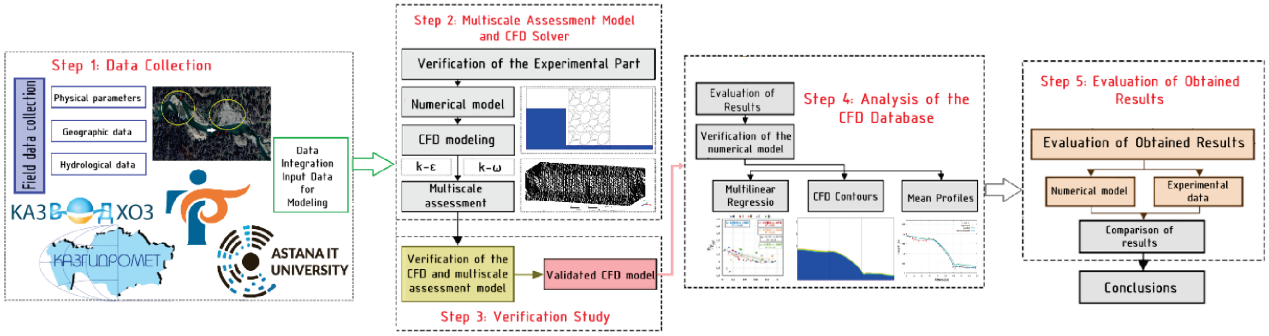

Figure 3. Conceptual diagram

VOF method

The Volume of Fluid Method (VOF) [14], [15], [16], [17] is used to track the movement and deformation of the interface between phases in multicomponent flows. This technique introduces a scalar function of the volume fraction of liquid, α, which indicates what part of the grid cell volume is filled with water (or another liquid). The value $\alpha = 1$ means that the cell is completely occupied by liquid, $\alpha = 0$ — completely by gas, and $0 < \alpha < 1$ indicates interface cells. The evolution of α is described by the transport equation

$$\frac{\partial \alpha}{\partial t} + \nabla(\alpha u) = 0 \tag{1}$$

which ensures the transfer of the volume fraction of liquid along with the flow. The physical properties of the mixture (density ρ and viscosity μ) are calculated as weighted by α:

$$\rho = \alpha\rho_{water} + (1-\alpha)\rho_{air} \tag{2}$$

$$\mu = \alpha\mu_{water} + (1-\alpha)\mu_{air} \tag{3}$$

The VOF model allows the shape and motion of the free surface to be accurately reproduced and also takes into account surface tension effects where necessary.

Mathematical model

To build a mathematical model, the laws of conservation of mass and momentum are used for an incompressible viscous isothermal fluid in the absence of mass and surface forces, as well as a system of Reynolds-averaged Navier-Stokes equations [18]:

$$\nabla \boldsymbol{u} = 0 \tag{4}$$

$$\frac{\partial}{\partial t}(\rho u_i) + \frac{\partial(\rho u_i u_j)}{\partial x_j} = -\frac{\partial p}{\partial x_i} + \frac{\partial \tau_{ij}}{\partial x_j} + S_i^{Por} + \rho g_i \tag{5}$$

where, $\boldsymbol{u} = (u, v, w)$ – is velocity components, ρ – is fluid pressure; μ – is dynamic viscosity, ρ – is liquid density, $\tau_{ij} = \mu\left(\frac{\partial u_i}{\partial x_j} + \frac{\partial u_j}{\partial x_i}\right)$ – is the mean tensor of viscous stresses, g_i – components of gravity.

$$S_i^{Por} = \frac{\mu}{K} u_i - \frac{1}{2}\rho C_2 |\boldsymbol{u}| u_i \tag{6}$$

where, K – permeability (Darcy), C_2 – is the Forchheimer coefficient.

Turbulence kinetic energy k and velocity and ε rate of dissipation are determined from the transfer equation:

DOI: 10.37943/23FVQL2644

$$\frac{\partial(\rho k)}{\partial t} + \nabla(\rho k \boldsymbol{u}) = \nabla\left[\left(\mu + \frac{\mu_t}{\sigma_k}\right)\nabla k\right] + G_k - \rho\varepsilon \quad (7)$$

$$\frac{\partial(\rho\varepsilon)}{\partial t} + \nabla\rho\varepsilon\mathbf{u} = \nabla\left[\left(\mu + \frac{\mu_t}{\sigma_\varepsilon}\right)\nabla\varepsilon\right] + C_{1\varepsilon}\frac{\varepsilon}{k}G_k - \rho C_{2\varepsilon}\frac{\varepsilon^2}{k} \quad (8)$$

where, $\mu_t = \rho C_\mu \frac{k^2}{\varepsilon}$ is turbulent viscosity, $G_k = \mu_t\left(\frac{\partial u_i}{\partial x_j} + \frac{\partial u_j}{\partial x_i}\right)\frac{\partial \overline{u_i}}{\partial x_j}$ is the rate of turbulence energy generation in the middle current. The coefficients of the model have the following standard values: $C_\mu = 0.09$, $C_{\varepsilon^1} = 1.44$, $C_{\varepsilon^2} = 1.92$, $\sigma_k = 1.0$, $\sigma_\varepsilon = 1.3$.

Numerical simulation algorithm

As is known, the PISO (Pressure-Implicit with Splitting of Operators) algorithm is used to solve unstable hydrodynamic problems in ANSYS Fluent [19], which is widely used in numerical integration of the Navier-Stokes equations. The PISO numerical algorithm allows for effective and stable coupling of pressure and velocity fields, which is especially important when modeling rapidly changing non-stationary flows [20]. This algorithm consists of two cycles, such as predictor and corrector steps, in the following form:

Predictor Step: The expected pressure field p^* is specified. Then, given this value of the solution to the discretized momentum equation, the preliminary velocities (u^* = u^*, v^*) are calculated.

Corrector Step 1: Corrections to the pressure field $\mathbf{u}^* = (u^*, v^*)$ are calculated based on the violation of the continuity equation by the obtained velocities. Next, the pressure $p^{**} = p^*, \delta p^{(1)}$ is updated and then the velocity components $\mathbf{u}^* = \boldsymbol{u}^*, +\delta\boldsymbol{u}^{(1)}$, where $\delta\boldsymbol{u}^{(1)}$ are related to $\delta p^{(1)}$.

Corrector Step 2: At this stage, additional corrections are made to eliminate the remaining discrepancies:

$$\delta p^{(2)} = p^*, +\delta p^{(1)}, \quad (9)$$

$$p^{***} = p^{**} - \delta p^{(2)} \quad (10)$$

$$\mathbf{u}^{***} = \mathbf{u}^{**}, +\delta\boldsymbol{u}^{(2)}, \quad (11)$$

where, $\delta\boldsymbol{u}^{(2)}$ are calculated similarly to the first correction step.

Therefore, after completing both steps, the required accuracy of the continuity equation and the equations of motion is achieved. If necessary, PISO iterations can be repeated until the specified convergence criteria for the residuals are achieved. Thus, this approach helps to provide a faster and more reliable matching of pressure and velocity fields than the classical SIMPLE scheme, which is why PISO is the standard for unsteady flow calculations in ANSYS Fluent.

Numerical test case validation Lin, 1999

The presented test problem is to check the numerical model by comparing the results with the experimental data given in the work (Lin, 1999, [13]). The experimental studies were carried out in a setup with dimensions of $0.892\ \text{m} \times 0.37\ \text{m} \times 0.44\ \text{m}$, and the dimension of the porous structure was $0.29\ \text{m} \times 0.37\ \text{m} \times 0.44\ \text{m}$ and was located at a distance of 0.3-0.59 m along the X-axis. The numerical simulation begins with the opening of the vertical gate, after which the water flow moves along the channel. Other details of the experiment can be found in the study (Lin, 1999, [13]). Figure 4 shows the complete scheme of the computational domain. In order to prevent water splashes from falling on the porous region, the height of the water reservoir was 25 cm. In order to compare the computational results and the experiment, 1.4 seconds were enough for the simulation.

Scientific Journal of Astana IT University
ISSN (P): 2707-9031 ISSN (E): 2707-904X
VOLUME 23, SEPTEMBER 2025

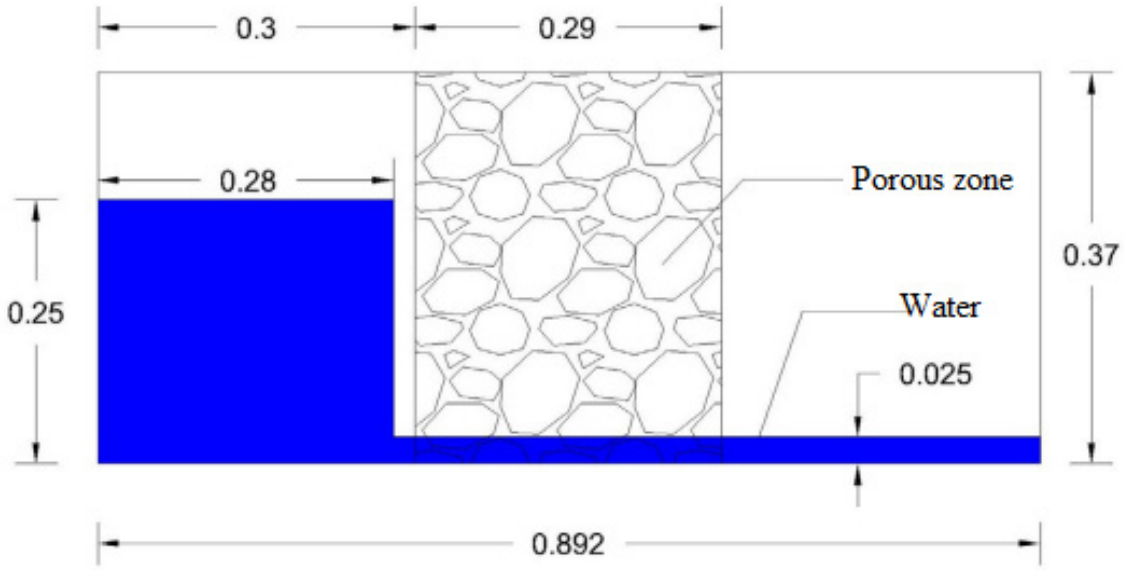

Figure 4. Computational domain of the test case

The boundary conditions were set as follows for the physical model: on the solid walls of the channel – non-slip walls, the upper boundary of the region was considered open and atmospheric pressure was set.

The total number of elements in the grid is 3,919,182. dmax = 0.10612 m, and dmin = 5.306e-004 m, time step dt = 0.01 s.

Results and Discussion

The obtained results of the numerical experiment showed that the developed model successfully reproduces the main characteristics of the flow observed in the experiment [13]. The evolution of the free water surface height over time for the control points of the experiment and calculation is shown (Figure 5). It is evident that the graphs of the numerical and experimental level changes practically coincide, which indicates a high accuracy of the model. In particular, the time of filling the porous insert with water and the rate of level rise at the entrance to the porous region in the calculation corresponds to the measured values. The maximum water height in front of the porous barrier, achieved after opening the gate, is also close to that recorded in the experiment. Small discrepancies appear only at later stages, can be noticed after 1 second of modeling and can be associated with turbulent pulsations, measurement inaccuracy or the influence of three-dimensional effects. In general, the coincidence of the calculated and experimental curves confirms the adequacy of the selected model parameters and numerical methods.

Also shown are successive two-dimensional images of the flow movement process through the porous insert, the presented images are obtained from a 3D calculation, displaying the central section of the channel (Figure 6). These visualizations illustrate the propagation of the breakthrough wave along the channel and its interaction with the porous obstacle. After the gate opens, the water flow quickly fills the area in front of the porous obstacle, forming a surge of water upstream from it. Then the water begins to leak through the porous structure: the flow front inside the insert moves more slowly than in a free channel and is noticeably slowed down due to the resistance of the material.

DOI: 10.37943/23FVQL2644

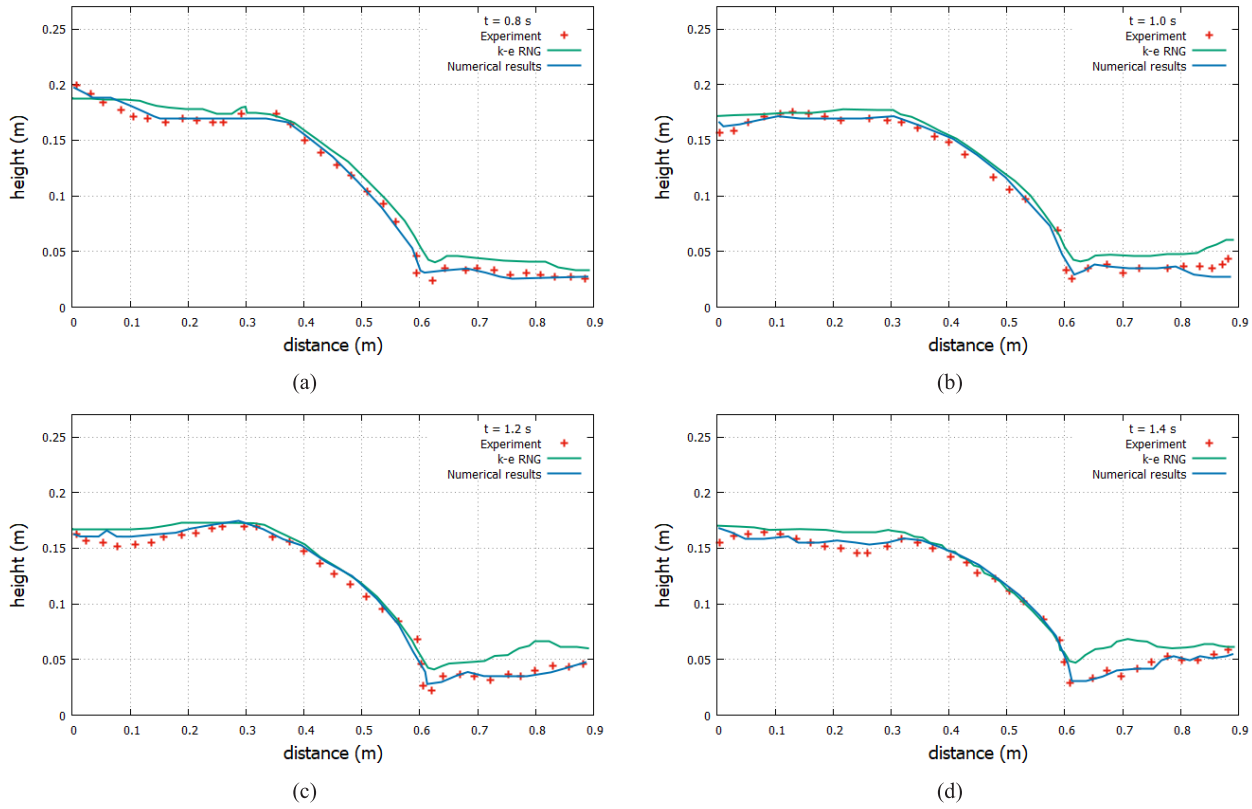

Figure 5. Water height throughout the simulation process:
(a) t=0.8 sec, (b) t=1.0 sec, (c) t=1.0 sec, (d) t=1.4 sec.

By the end of the calculation, the water completely penetrates the porous barrier and flows into the lower part of the channel, but its speed and depth are significantly reduced compared to the case without a barrier. These numerical flow patterns are in qualitative agreement with experimental observations [13]: in both cases, the porous block acts as an energy absorber, reducing the height and speed of the wave due to filtration. Note that performing the calculation in a three-dimensional formulation made it possible to take into account the possible uneven distribution of the flow across the width of the channel, which cannot be achieved in 2D models. Nevertheless, in this case, the flow turned out to be almost uniform in width, due to which the two-dimensional sections quite fully reflect the nature of the process (Figure 5).

Scientific Journal of Astana IT University
ISSN (P): 2707-9031 ISSN (E): 2707-904X
VOLUME 23, SEPTEMBER 2025

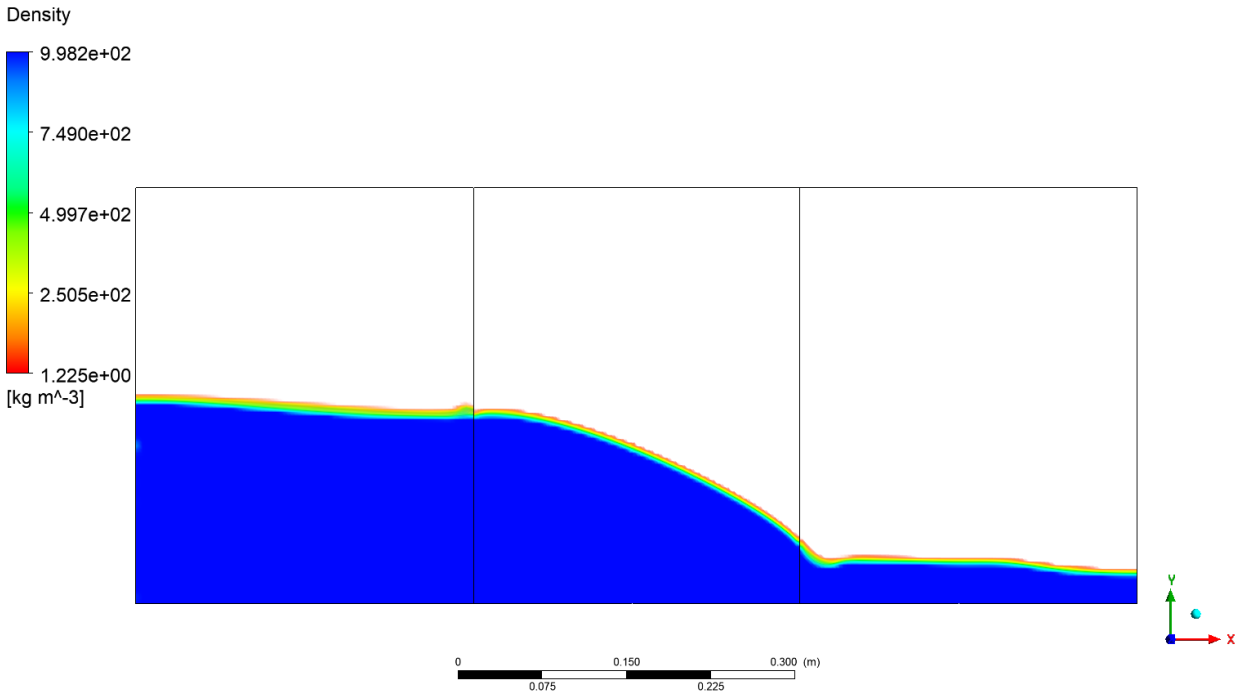

(a)

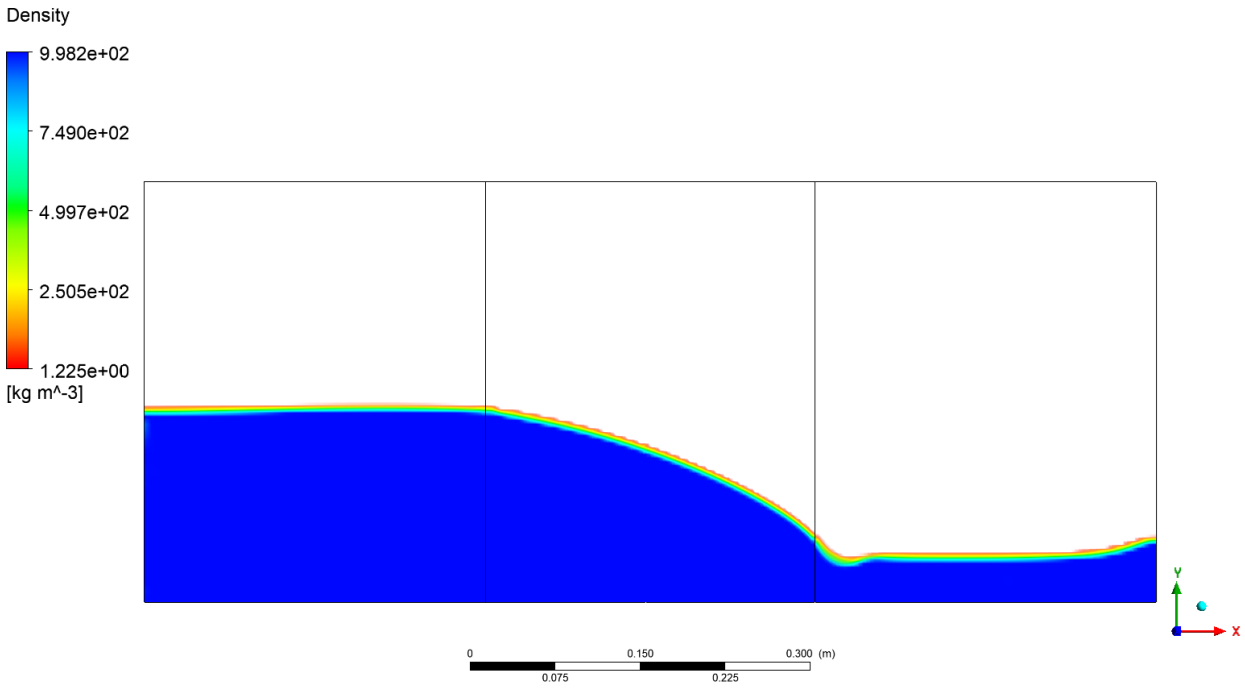

(b)

DOI: 10.37943/23FVQL2644

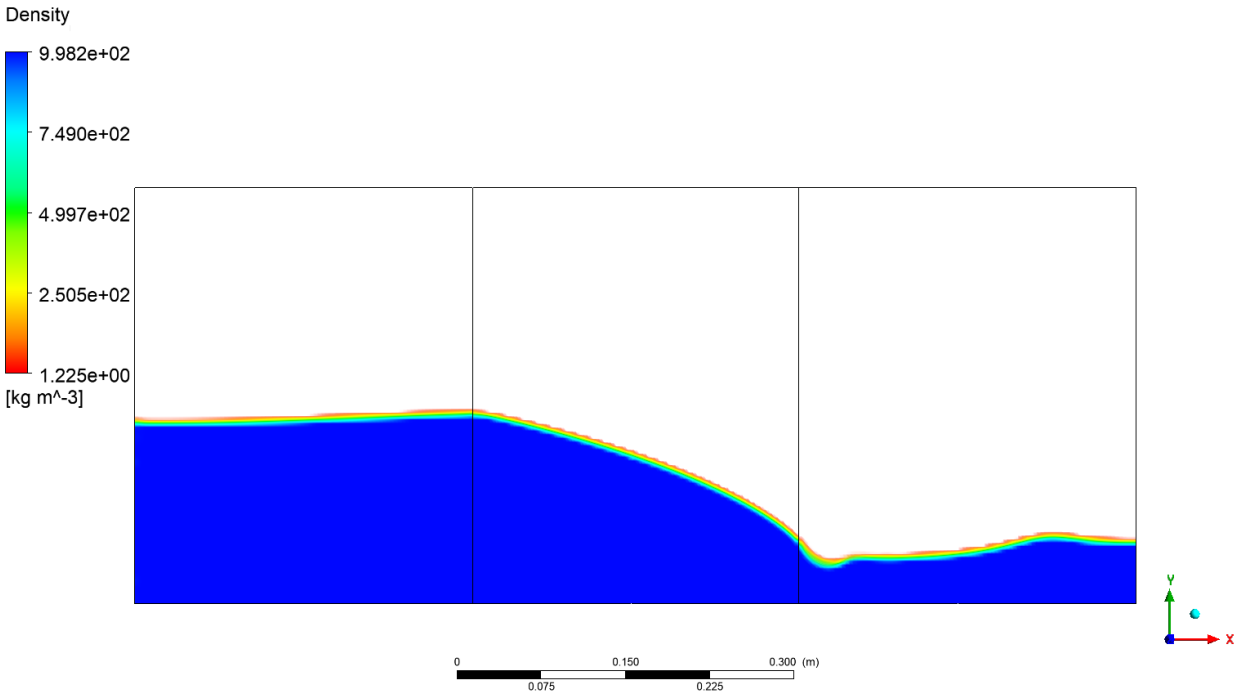

(c)

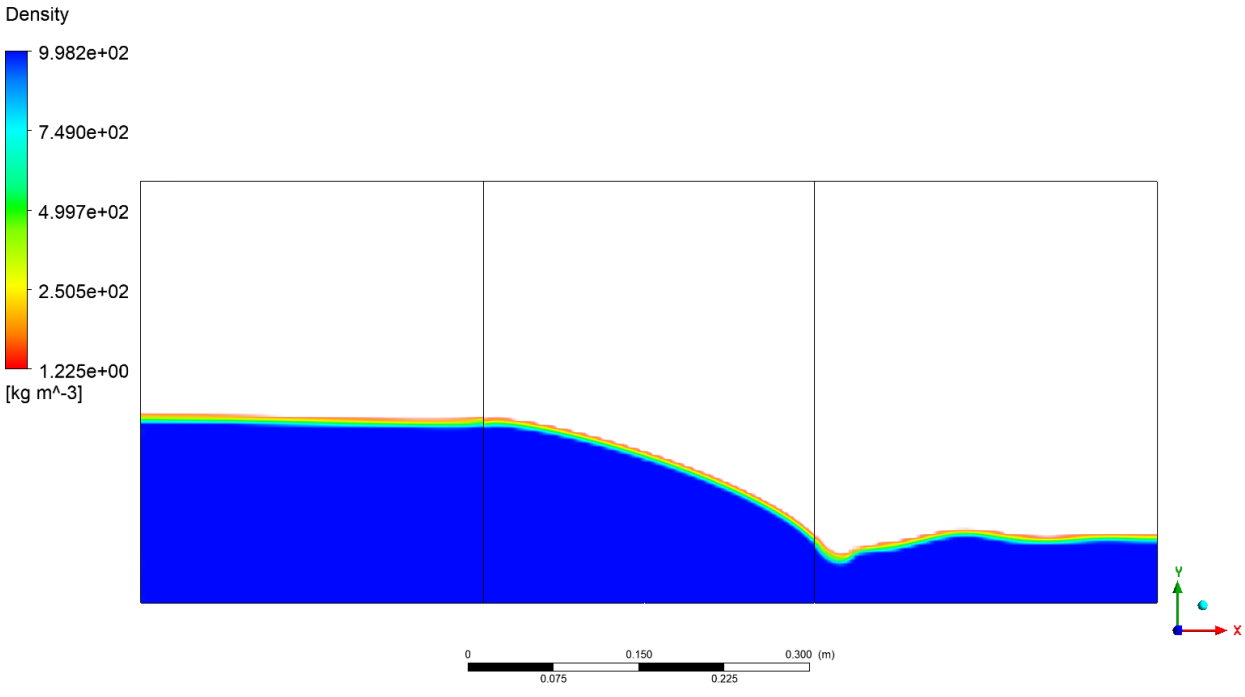

(d)

Figure 6. Two-dimensional images of the process of water flow through a porous region

Scientific Journal of Astana IT University
ISSN (P): 2707-9031 ISSN (E): 2707-904X
VOLUME 23, SEPTEMBER 2025

Conclusion

In the presented work, a three-dimensional numerical model of water flow through a porous medium was implemented and verified, where the reliability of the data is based on a laboratory experiment [13]. Thus, a comparison of the change in water and velocity with laboratory data showed that the discrepancies do not exceed 5%. Also, the selected methods – the VOF model for the free surface, the RNG version of the turbulent k-ε model and the PISO algorithm for the pressure-velocity relationship – adequately describe the physical picture of the experiment. The parameters of the porous zone – the porosity value φ, the permeability k and the inertial coefficient C2 – were also correctly selected.

The obtained results describe how the propagation of the shock wave of the penetration and its interaction with the porous barrier are reproduced (Figures 5, 6). As a result, then quickly fills the box before insertion and then only slows down, and the presence of a porous medium partially filters through the pores and leads to a noticeable decrease in the depth and flow velocity in the underlying part of the channel. Thus, this three-dimensional model made it possible to verify the homogeneity of the flow across the width, confirming that two-dimensional sections sufficiently fully reflect the key hydrodynamic mechanisms. This kind of laboratory tasks helps to create a solid basis for transferring the model to the real conditions of the Talas River, which is planned to adapt the calculation area to the natural channel profile, set field hydrographs and porosity parameters of the "jam" zones, and then conduct similar comparisons with field measurements of level and velocity. It is worth noting that the resulting numerical platform will be useful for predicting flood processes, assessing erosion and sediment accumulation, as well as for developing an early warning system for environmental risks and planning measures to protect water resources.

This integrated approach provides a robust tool for hydrologists, ecologists and engineers to combine a detailed physical flow model with practical river monitoring and management tasks.

Acknowledgement

This research was funded by the Science Committee of the Ministry of Science and Higher Education of the Republic of Kazakhstan, grant number BR24993128 “Information-analytical system development for the transboundary water resources effective use in the Zhambyl region agricultural sector.”

References

[1] Champness, M., Vial, L., Ballester, C., & Hornbuckle, J. (2023). Evaluating the performance and opportunity cost of a smart-sensed automated irrigation system for water-saving rice cultivation in temperate Australia. Agriculture, 13(4), 903. https://doi.org/10.3390/agriculture13040903

[2] Simsek, O., & Islek, H. (2023). 2D and 3D numerical simulations of dam-break flow problem with RANS, DES, and LES. *Ocean Engineering, 276*, 114298. https://doi.org/10.1016/j.oceaneng.2023.114298

[3] Kreibich, H., Van Loon, A.F., Schröter, K., et al. (2022). The challenge of unprecedented floods and droughts in risk management. Nature, 608, 80–86. https://doi.org/10.1038/s41586-022-04917-5

[4] Rentschler, J., Salhab, M., & Jafino, B.A. (2022). Flood exposure and poverty in 188 countries. Nature Communications, 13, 3527. https://doi.org/10.1038/s41467-022-30727-4

[5] Zhou, X., Su, L., He, X., Hu, R., & Yuan, H. (2024). Experimental investigations of propagation characteristics and wave energy of dam-break waves on wet bed. Ocean Engineering, 301, 117566. https://doi.org/10.1016/j.oceaneng.2024.117566

[6] Vosoughi, F., Nikoo, M.R., Rakhshandehroo, G., & Gandomi, A.H. (2021). Experimental dataset on water levels, sediment depths and wave front celerity values in the study of multiphase shock

wave for different initial up- and down-stream conditions. *Data in Brief*, 36, 107082. https://doi.org/10.1016/j.dib.2021.107082

[7] Rodrigues, J.M., Lavrov, A., Hinostroza, M.A., & Guedes Soares, C. (2018). Experimental and numerical investigation of the partial flooding of a barge model. *Ocean Engineering, 169*, 586–603. https://doi.org/10.1016/j.oceaneng.2018.09.042

[8] Ozmen-Cagatay, H., Turhan, E., & Kocaman, C. (2022). An experimental investigation of dam-break induced flood waves for different density fluids. Ocean Engineering, 243, 110227. https://doi.org/10.1016/j.oceaneng.2021.110227

[9] Khosravi, K., Chegini, A.H.N., Cooper, J. R., Mao, L., Roshan, M.H., Shahedi, K., & Binns, A.D. (2020). A laboratory investigation of bed-load transport of gravel sediments under dam break flow. International Journal of Sediment Research. https://doi.org/10.1016/j.ijsrc.2020.08.005

[10] Ma, C., Peng, M., Zhang, L., Shi, Z., Zhou, J., Chen, H., Zhu, Y., & Li, Z. (2024). Erosion, deposition and breach evolution of landslide dams composed of various dam material types based on flume tests. Engineering Geology, 337, 107598. https://doi.org/10.1016/j.enggeo.2024.107598

[11] Xu, H., & Cao, Z. (2024). Experimental study of reservoir flushing through a bottom tunnel initially covered by cohesive sediment. International Journal of Sediment Research, 39(3), 327–339. https://doi.org/10.1016/j.ijsrc.2024.03.004

[12] Erduran, K. S., Ünal, U., & Dokuz, A. S. (2024). Experimental and numerical investigation of partial dam-break waves. Ocean Engineering, 308, 118346. https://doi.org/10.1016/j.oceaneng.2024.118346

[13] Dong, Y., Tan, W. H., Chen, H., & Yuan, J. (2024). Numerical modeling of wave interaction with a porous floating structure consisting of uniform spheres. *Physics of Fluids*, 36(7), 072107. https://doi.org/10.1063/5.022216

[14] Garoosi, F., Kantzas, A., Irani, M. (2024). Numerical simulation of wave interaction with porous structure using the coupled Volume-Of-Fluid (VOF) and Darcy-Brinkman-Forchheimer model. *Engineering Analysis with Boundary Elements, 166,* 105866. https://doi.org/10.1016/j.enganabound.2024.105866

[15] Li, B., Ma, H. (2025). Numerical model for sediment transportation under breaking wave: The application exploration of VOF-CFD-DEM model in gas-fluid-particle system. *Computers and Geotechnics, 177, Part A,*106844. https://doi.org/10.1016/j.compgeo.2024.106844

[16] Meng, W., Yu, C., Li, J., Wu, Z., An, R. (2025). Modeling of interfacial two-phase flows via VOF-based LS method with WENO scheme in the finite volume method. *Computers & Fluids, 291,* 106580. https://doi.org/10.1016/j.compfluid.2025.106580

[17] Yan, S., Zhang, X., Luo, Z. (2025). Adaptive mesh refinement for VOF modeling gas-liquid two-phase flow: A summary of some algorithms and applications. *Chemical Engineering Science, 306,* 121291. https://doi.org/10.1016/j.ces.2025.121291

[18] Caramia, G., Amirante, R., De Palma, P. (2024). Unsteady RANS simulations of under-expanded hydrogen jets for internal combustion engines. *International Journal of Hydrogen Energy, 96,* 849-859. https://doi.org/10.1016/j.ijhydene.2024.11.242

[19] Paras, S., Kumar, A. (2024). ANSYS Fluent-CFD analysis of a continuous single-slope single-basin type solar still. *Green Technologies and Sustainability, 2(3),* 100105. https://doi.org/10.1016/j.grets.2024.100105

[20] Fanxi, B., Liu, Y., Liu, Y., Xu, Z., Chen, S., Jiang, M. M., & Guan, B. (2021). Leakage diffusion characteristics and harmful boundary analysis of buried natural gas pipeline under multiple working conditions. *Journal of Natural Gas Science and Engineering*, 88, 104047. https://doi.org/10.1016/j.jngse.2021.104047